FORC Analysis of Nanopatterned vs. Unpatterned Films: Coercivity and Switching Mechanisms

Alecsander D. Mshar^{1, a)}, Allen G. Owen¹, Daniel D. Arnold², Pieter B. Visscher³, Randy K. Dumas⁴, Subhadra Gupta⁵

¹Electrical and Computer Engineering, University of Alabama, Tuscaloosa, AL, United States

²Computer Science, University of Alabama at Huntsville, Huntsville, AL, United States

³Physics and Astronomy, University of Alabama, Tuscaloosa, AL, United States.

⁴Quantum Design, San Diego, CA, United States

⁵Metallurgical and Materials Engineering, University of Alabama, Tuscaloosa, AL, United States

a) Author to whom correspondence should be addressed: admshar@crimson.ua.edu

We have studied the use of self-assembled block copolymers to pattern multilayers of Co and Pd on silicon wafers. Stacks ranging from four to twelve bilayers of Co (0.3 nm)/Pd (0.8 nm) were sputtered onto Ta/Pd seed layers and capped with 3 nm of Ta and were found to have perpendicular magnetic anisotropy asdeposited. The block copolymer polystyrene-block-poly(ferrocenyl dimethylsilane) (PS-b-PFS) was dissolved in toluene and spun onto the wafers. The polymers were phase-separated by heat treatment, leaving self-assembled PFS spheres embedded in PS, which was removed by oxygen-plasma ashing. The PFS spheres were then used as masks to ion-mill the Co/Pd multilayers into nanopillars. To study the effect of etch time and etch angle on the coercivity distribution, we synthesized samples in a Design of Experiments-(DoE)- in these two factors. Scanning electron micrographs showed nanopillars ranging from 15 to 30 nm in diameter, depending primarily on etch time. M-H loops measured on both patterned and unpatterned wafers showed an increase of up to 130% in overall coercivity upon patterning. First Order Reversal Curves (FORC) were measured, and the resulting FORC distributions displayed using a smoothing program (FORCinel) and one that can display the raw data without smoothing (FORC+). We find that FORC+ reveals information about fine-scale structure and switching mechanism that cannot be seen in the smoothed display.

I. INTRODUCTION

Bit patterned media (BPM) is a promising technology that has the potential to increase current digital media storage density. Perpendicular magnetic anisotropy materials (PMA) are used to decrease the interactions between individually patterned bits, allowing the density of these bits to increase while still maintaining the magnetic properties necessary for the material to be viable as magnetic storage media.

The block copolymer nanopatterning process^{1,2,3} forms self-assembled nanospheres on the surface of a film by phase-separating the two polymers. Once separated, one of the polymers (PS) is removed in an oxygen plasma environment. This leaves behind the other polymer (PFS), which has self-assembled into spheres during the phase separation. These spheres

are then used as masks in an ion-mill etching process to transfer the pattern to the underlying PMA Co/Pd multilayer film. This forms a distribution of PMA nanopillars whose size depends on the etching conditions used.³ Smaller nanopillar diameters correspond to higher coercivity and reduce the magnetic interactions between bits.

In this paper the block copolymer nanopatterning process was used to pattern three magnetic film stacks of different structure. The films were PMA Co/Pd multilayers deposited with four, eight, and twelve bilayers of Co/Pd. The films were then imaged with a scanning electron microscope (SEM) and measured with a vibrating sample magnetometer (VSM). The SEM data shows the physical structure of the nanopillars at various stages in the process. The VSM data produced both M-H

loops and first order reversal curve (FORC) measurements to study the magnetic properties and magnetization switching of the materials.

II. FILM DEPOSITION

Three variations of a Co/Pd multilayer film stack were deposited on three-inch Si substrates using a Sputtered Films Inc. Shamrock planetary sputtering system. Full wafers with films of four, eight, and twelve Co/Pd bilayers were deposited in separate processes. Each layer of the films was sputtered using a DC magnetron cathode at an Ar process pressure of 0.26 Pa. Each bilayer consisted of 0.3 nm of Co and 0.8 nm of Pd. The film stacks with eight and twelve multilayers were seeded with 10 nm of Ta and 5 nm of Pd. The four-bilayer film stack was seeded with 15 nm of Ta and 5 nm of Pd to increase the overall thickness of the final stack. Each stack was then capped with a 3 nm layer of Ta. This process resulted in three wafers with stacks of the following compositions: Ta15/Pd5/[Co0.3/Pd0.8]x4/Ta3 nm; Ta10/Pd5/[Co0.3/Pd0.8]x8/Ta3 nm; Ta10/Pd5/[Co0.3/Pd0.8]x12/Ta3 nm. The final thicknesses of these film stacks were then measured using a Dektak profilometer.

Each of these three wafers was cut into two parts, one part to be patterned using a block copolymer process and one part to leave unpatterned. The samples to be patterned were each spin coated with polystyrene-b-polyferrocenyldimethylsilane (PSb-PFS) using a Solitec spin-coater at 4000 rpm for 40s. The films were then baked at 140°C for 48 h on a hot plate. The baking process caused the block copolymer to phase-separate and form PFS spheres in a PS matrix. The films were then exposed to an oxygen plasma at 300 W for 1 min with an oxygen pressure of 133.3 Pa. This ashing process removed the PS and left behind a distribution of PFS spheres. The PFS spheres were then used as etch masks. The samples were ion milled with a Veeco ion source at 13 W at various etch angles and etch times. The etch angle (EA, between the incident Ar ion beam and the film plane) was varied from 35° to 55°. The etch time (ET) was varied from 2 min to 3 min. This process removed the exposed material and formed small pillars of Co/Pd multilayers.

A design of experiments (DoE) was constructed on Minitab to investigate the responses (coercivity and nanopillar diameter) to the factors of etch time and etch angle for the patterned samples. A total of 10 samples were processed in this DoE. The samples were all cut from the same wafer so that each sample had identical deposition and spin coating parameters, as well as ashing conditions. The samples were then ion milled at etch times and angles determined using a 2-factor full central composite DoE with an α value of 1.

The out-of-plane M-H hysteresis loop of each patterned and unpatterned sample was measured using a Quantum Design Dynacool Physical Property Measurement System VSM module. Several samples were also imaged using a ThermoFisher Apreo SEM to determine the average diameters of the PFS masks and final nanopillars.

III. FORC MEASUREMENTS

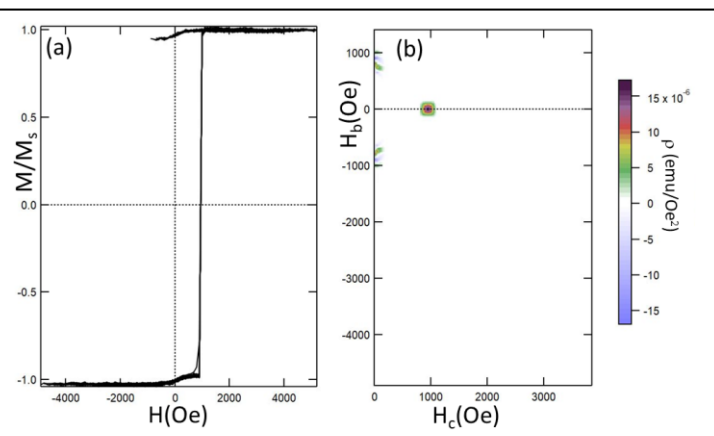


Fig. 1. (a) FORC curves M(H,HR) of unpatterned 12-bilayer film, (b) the FORC distribution $\rho(H,HR) = -\frac{1}{2} \partial^2 M(H,HR)/\partial H\partial H_R$, using the FORCinel averaging program⁴ with the default smoothing factor of 4. There is one peak of unresolvable width. The streaks near $H_b = \pm 600$ -900 Oe and $H_c = 0$ are artifacts due to smoothing (they are not present in the unsmoothed FORC+ display).

Fig. 1(a) shows the FORC curves of the unpatterned 12-bilayer sample. Each of these FORCs is produced by first saturating the sample positively, then reducing the magnetic field H to a "reversal field" $H_{\rm R}$. From there, H is increased slowly and $M(H,H_{\rm R})$ is recorded. In this particular case, many of the FORCs are on top of each other, so it is hard to distinguish them – the ones for the patterned film

(Fig. 3, below) are easier to distinguish. The hysteresis loop (the envelope of the FORC curves) is nearly rectangular, so the FORC density (shown in Fig. 1(b) using the smoothing program FORCinel⁴) has a very narrow peak, at coercivity $H_c \sim 950$ Oe and zero bias H_b. If our system is composed of Preisach hysterons, the density $\rho(H,H_R)$ can be interpreted as the total moment of the hysterons with switching fields H and H_R. In this instance, the system behaves almost like a single ideal Preisach hysteron with $H = H_c$ and $H_R = H_{\text{c}}\$ In this smoothed form, the FORC measurement is not useful, since the coercivity could have been determined from a simple hysteresis loop measurement. However, close examination of the FORC curves (Fig. 1(a)) reveals a deviation from this picture: at the lower right, at H ~ H_c, where the FORC

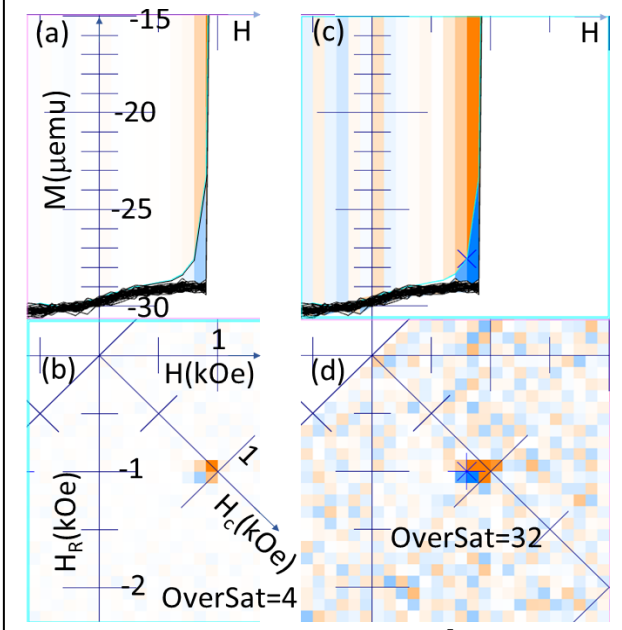


Fig. 2. The zoomed FORC+ display⁵ of the same unpatterned sample whose smoothed FORCinel display is shown in Fig. 1. (a) the FORC curves $M(H,H_R)$ and (b) the FORC distribution – the color (orange for positive, blue for negative) of each square plaquette is proportional to the FORC density $\rho(H,H_R)$. Each plaquette in (b) maps to a trapezoid directly above it in (a). To help the reader see this correspondence, FORC+ has filled the trapezoid with the same color as the corresponding plaquette. Parts (c,d) show the same information as (a,b) with a much larger oversaturation (32 vs. 4). The "x" is a movable cursor at the H_R = -1000 Oe FORC curve, showing its position in the density display.

curve switches back up, one of the curves starts switching up before the others. Fig. 2(a) shows an enlarged (zoomed) picture of this region, using the unsmoothed FORC+ display program⁵. The FORCs with $H_R \geq -900$ Oe never switch down, hence are not visible in this zoomed view. The highest FORC that is visible (the one that "cuts the corner" at the lower right) has $H_R = -1000$ Oe. The next one ($H_R = -1100$ Oe) is almost indistinguishable from the lower ones (-1200, -1300, etc.)

This behavior has a simple physical interpretation 7,8 . The identical FORCs (with $H_R = -1100, -1200, ...$) are identical because they completely saturate in the negative direction at H_R . The one at $H_R = -1000$ Oe reverses, but does not completely saturate — there are a few unswitched "holdout" areas that can act as nuclei for re-reversal. Thus rereversal occurs at a lower field, and this curve slopes upward before the saturated curves do.

In Fig. 2(b), we show a color map of the FORC density $\rho(H,H_R) = -\frac{1}{2} \ \partial^2 M(H,H_R)/\partial H\partial H_R$, using the FORC+ display program⁵. The discrete crossed partial derivative is simply a sum (with alternating signs +,-,+,-) of the values of M at the corners as one goes around the plaquette. The brightness of the orange color in this plaquette is proportional to the value of ρ if $\rho \ge 0$; if $\rho < 0$ the blue brightness is $\rho = |\rho|$. To make small densities more visible, we oversaturate the highest density – in Fig. 2(b), the oversaturation is 4, meaning that the highest-density (bright orange) plaquette is actually 4x higher than its color indicates. It is at least 10x higher than any other plaquette. Each plaquette in Fig. 2(b) corresponds uniquely to a trapezoid in Fig. 2(a), which has the same color.

The FORC+ display in Fig. 2(b) clearly shows the effect of the "holdout" phenomenon mentioned above – it leads to a negative (blue) region to the left of and below (i.e., in the negative-bias direction from) the main positive peak. Thus we **can** get information about the physics of the reversal from the FORC measurement, but it involves very fine structure in the H-H_R plane which is destroyed by averaging. We can get more information about the shape of the peak if we increase the color scale ("oversaturation"), which is 4 in Fig. 2(b). In Fig. 2(c,d) we show the same peak with oversaturation 32 – we can better see the position of the negative region relative to the positive

peak, at the cost of concealing the huge difference in intensity: the total weight of the positive peak is about 30 times larger than the negative one. Changing the oversaturation is very fast in FORC+ -- the display is created by direct calls to OpenGL functions (which are used to produce graphics in every modern computer architecture). The CPU sends the vertex data for thousands of triangles to the GPU only once — to change the oversaturation we need send only a single number.

The FORC density is plotted in the H-H_R plane in Fig. 2 (b,d), but we also draw the axes for coercivity $H_c = \frac{1}{2}(H - H_R)$ and bias field $H_b = \frac{1}{2}(H + H_R)$.

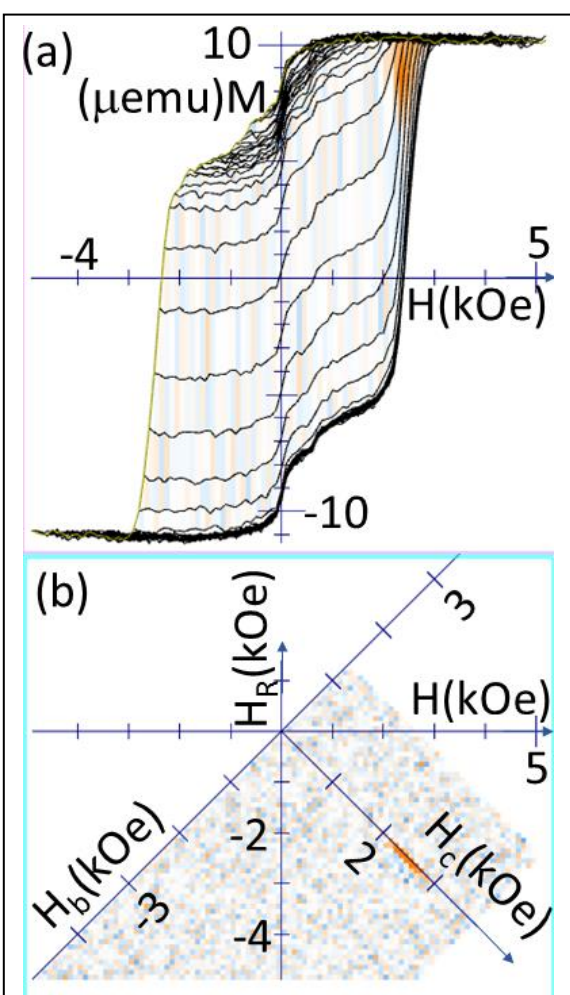


Fig. 3. (a) FORC curves for the patterned sample etched for 2.5 min at 35°, (b) FORC+ display of the FORC density, using oversaturation = 2. Only one feature emerges from the noise, a peak near H_c = 2.5, shown in more detail in Fig. 4.

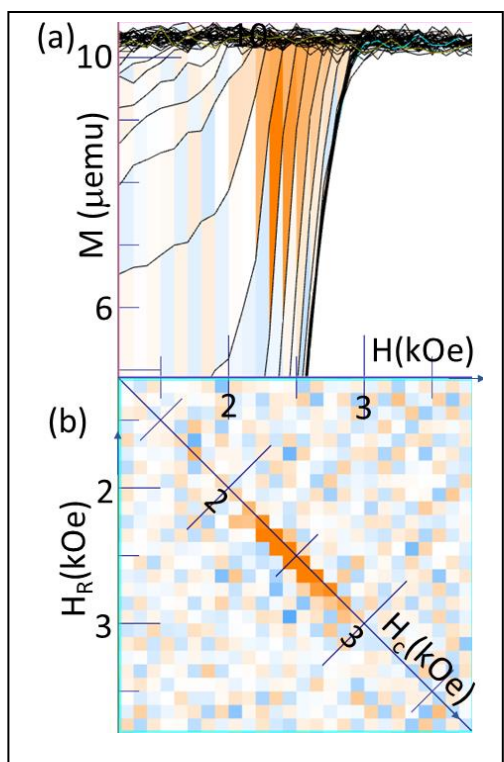


Fig. 4. Zoomed view in FORC+ of the FORC curves (a) and FORC density (b) for the patterned film in Fig. 3.

In Fig. 3, we show the FORC results for the patterned sample etched 2.5 minutes at 35°. There is only one non-noise feature in the FORC density, a peak at zero bias and $H_{\rm c}$ =2.5 kOe. We zoom in on this feature in Fig. 4, which shows that it is extremely narrow in the bias direction, essentially just one pixel (plaquette) wide.

It is important to recognize that the unsmoothed FORC+ display causes no loss of information – from FORC color map $\rho(H,H_R)$, which is the second discrete derivative of the raw data $M(H,H_R)$, and the first derivative (which FORC+ also displays as the 'reversible switching field distribution') we may recover $M(H,H_R)$ exactly by summation⁶. Although some FORC maps have smooth lowamplitude structure that is hard to distinguish from the noise without smoothing, in many cases, including the present one, all significant structures are readily seen in the unsmoothed FORC+ display.

IV. RESULTS AND DISCUSSION

Fig. 1 shows that the unpatterned 12-multilayer film has high perpendicular anisotropy and a

coercivity of about 1 kOe. After patterning by the block copolymer process and etching for 2.5 min at a 35° angle, the film retains its high perpendicular anisotropy and its coercivity increases by 130% to about 2.3 kOe, as seen in Fig. 3.

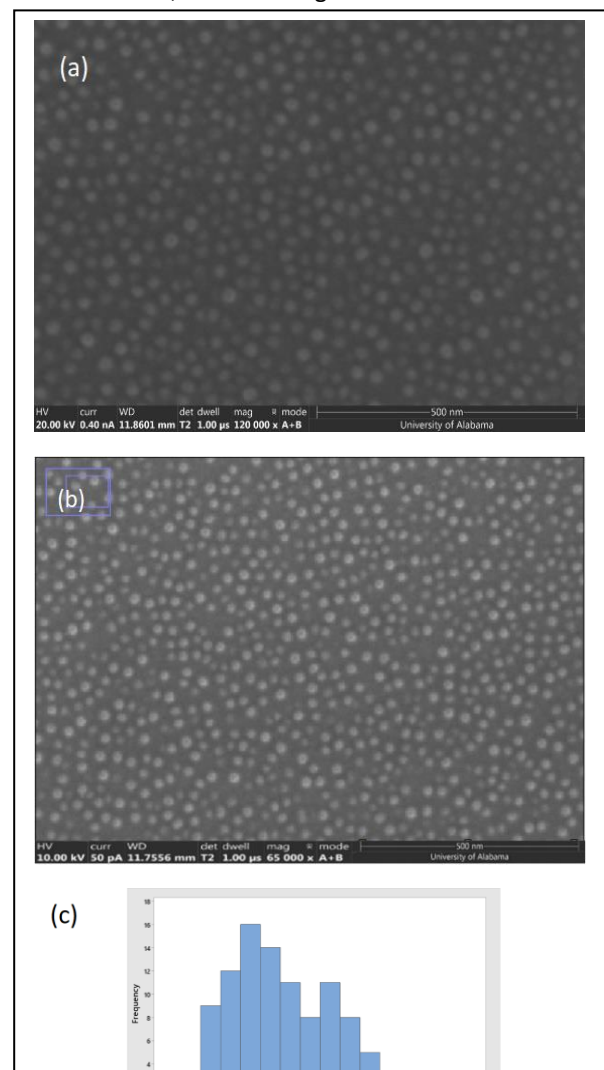


Fig. 5. SEM images of the [Co/Pd]x12 multilayer stack (a) after ashing, (b) nanopillars formed after etching, and (c) a histogram of the nanopillar diameter measurements taken from image (b).

Fig. 5 shows two SEM images. Image (a) was taken after the ashing step in the patterning process. The ashing process removes the PS polymer and leaves behind the previously formed PFS nanospheres. These spheres can clearly be seen in Fig. 5(a). The image in Fig. 5(b) was taken after the

sample was ion milled. The ion mill etches away the exposed material and forms nanopillars of the film stacks. The image processing software ImageJ was used to measure the diameters of the spheres and pillars; a histogram of the measured pillar diameters is shown in Fig. 5(c). One might expect this broad variation in pillar diameter to cause a large variation in coercivity, but in fact the relative coercivity variation seen in the FORC diagram (Fig. 4) is actually somewhat smaller than the variation in pillar diameter. The average diameter of the nanopillars is 21 nm, and that of the spheres in Fig. 5(a) is 22 nm. These are equal within experimental error, showing a faithful pattern transfer from the mask to the substrate.

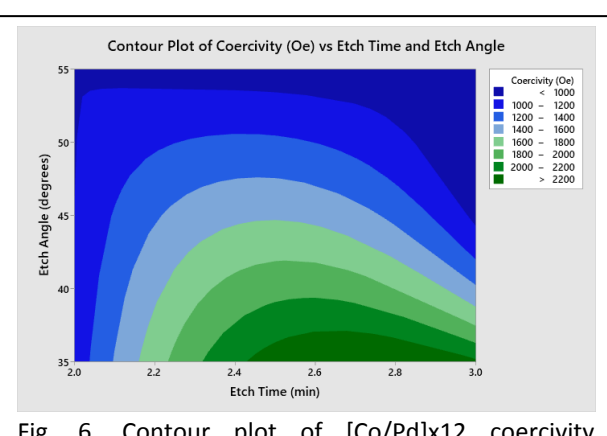


Fig. 6. Contour plot of [Co/Pd]x12 coercivity dependence on etch time and etch angle.

Fig. 6 shows a contour plot of the DoE results using the [Co/Pd]x12 multilayer film. The highest coercivity (2.3 kOe) was found in a sample that was ion milled for 2.5 minutes at an angle of 35°.

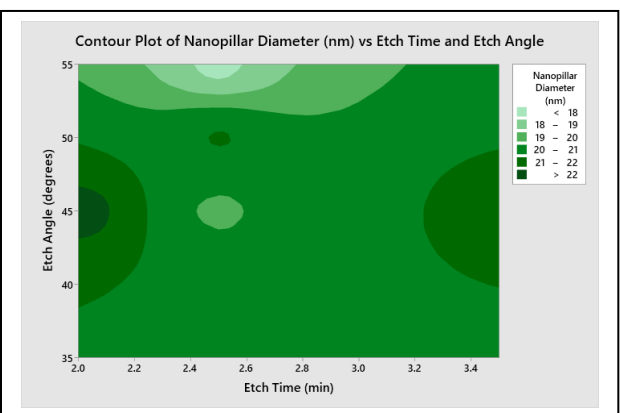


Fig. 7. Contour plot of [Co/Pd]x12 nanopillar diameter dependence on etch time and etch angle.

Fig. 7 shows the response of the nanopillar diameter of the DoE matrix for the [Co/Pd]x12 multilayer film. The smallest nanopillars were found in a sample that was milled for 2.5 minutes at 55°.

V. SUMMARY

In this paper we have optimized the coercivity of CoPd multilayer pillars with respect to the etch conditions: etching time and angle. We have also studied both patterned and unpatterned films using the FORC method and found that the fine structure of the FORC density can give information about switching mechanism that is inaccessible to smoothed display methods.

ACKNOWLEDGEMENTS

We acknowledge NSF ECCS 2053954 for support.

The FORC measurements were performed using a Quantum Design VersaLab PPMS in conjunction with the FORC software option for the VSM.

DATA AVAILABILITY STATEMENT

FORC data files and script files for producing Figs. 2-4 of this paper, as well as the FORC+ executable, are available at http://visscher.ua.edu/magvis/2022Intermag/.

REFERENCES

- ¹ T. Thomson, G. Hu, and B. D. Terris, Phys. Rev. Lett. 96, 257204 (2006).
- ² R. A. Griffiths, A. Williams, C. Oakland, J. Roberts, A. Vijayaraghavan, and T. Thomson, J. Phys. D: Appl. Phys. 46, 503001 (2013).
- ³ A. G. Owen, Hao Su, A. Montgomery and S. Gupta, J. Vac. Sci. Technol. B 35, 061801(2017).
- ⁴ https://wserv4.esc.cam.ac.uk/nanopaleomag/; R. J. Harrison and J. M. Feinberg, "FORCinel: An improved algorithm for calculating first-order reversal curve distributions using locally weighted regression smoothing", Geochem. Geophys. Geosyst., 9, Q05016(2008).
- ⁵ FORC+ program, http://MagVis.org.

- ⁶ P. B. Visscher, "Avoiding the zero-coercivity anomaly in first order reversal curves: FORC+", AIP Advances 9, 035117 (2019).
- ⁷ E. Davies, O. Hellwig, E. E. Fullerton, et al, "Magnetization reversal of Co/Pt multilayers: Microscopic origin of high-field magnetic irreversibility," Phys. Rev. B 70(22), 224434 (2004).
- ⁸ Joseph B. Abugri, P. B. Visscher, Subhadra Gupta, P. J. Chen and R. D. Shull, "FORC+ Analysis of Perpendicular Magnetic Tunnel Junctions", J. Applied Physics **124**, 043901 (2018).